Neuropsychiatry

Original article

DOI: https://doi.org/10.5114/nan.2022.117950

Statistical shape analysis of corpus callosum in functional neurological disorder

Murat Baykara[1], Sema Baykara[2], Murad Atmaca[2]

[1]Department of Radiology, Faculty of Medicine, Firat University, Elazig, Turkey
[2]Department of Psychiatry, Faculty of Medicine, Firat University, Elazig, Turkey

Neuropsychiatria i Neuropsychologia 2022; 17, 1–2: 1–8

Address for correspondence:
Doc. Dr. Murat Baykara
Firat Universitesi Tip Fakultesi Radyoloji A.D.
Elazig, Turkey
phone: +90 4242333555-1342
e-mail: muratbaykara@hotmail.com

Abstract

Introduction: Functional neurological disorder (FND) is the presence of neurological symptoms in the absence of a neurological disease. Diseases can cause degenerative changes in brain structures such as the corpus callosum (CC). Studies have shown that abnormalities in the CC are associated with FND symptoms. The aim of this study is to evaluate the CC of patients with statistical shape analysis (SSA) and compare it with that of healthy subjects.
Material and methods: Twenty patients with FND and 20 healthy individuals of similar ages, all females, participated in the study. In mid-sagittal images of each individual, the CC was marked using landmarks. The mean of 'Procrustes' points was calculated and shape deformations were evaluated using thin plate spline analysis.
Results: Significant differences in shape were observed in the CC between the two groups, with maximum CC deformation in posterior region markings in those with FND. There was no significant difference between the CC area of patients diagnosed with FND and controls.
Conclusions: Corpus callosum analysis with SSA revealed significant differences between patients and healthy subjects. The study findings highlighted the abnormal distribution of white matter in the CC and the variable subregional nature of CC in FND patients. This study may help future studies in terms of FND etiology, diagnosis and treatment options.

Key words: conversion disorder, somatoform disorders, corpus callosum, spatial analysis, image processing, computer-assisted.

Introduction

Functional neurological disorder (FND) is the presence of neurological symptoms in the absence of a neurological disease and the dysfunction defined for its diagnosis should not be associated with any medical disorder (American Psychiatric Association 2013; Aybek *et al*. 2015). Diagnostic criteria include the presence of one or more changes in volitional, motor, or sensory functions that may explain this appearance, and discordance and inconsistency between neurological or general medical conditions (American Psychiatric Association 2013). Although the findings reported in structural and functional neuroimaging studies in the literature do not adequately explain the pathophysiology of FND, some studies suggest and support the existence of important findings accompanying FND symptoms. These findings have led to an emphasis on disorders associated with FND symptoms that can be identified by neuroimaging and neurophysiological measurements (Aybek *et al*. 2015; Byrd *et al*. 1990; Vuilleumier *et al*. 2001; Atmaca *et al*. 2006; Giedd *et al*. 2012; Baumann and Mattingley 2012; Atmaca *et al*. 2016; Baykara *et al*. 2021; Baykara and Baykara 2021).

Neurological diseases can cause degenerative atrophic changes in any part of the brain and cause texture, size and shape changes especially in these regions (plasticity). It is possible that these changes alter the size and shape by causing changes in the structure of the corpus callosum (CC), which is the major white matter structure connecting the brain hemispheres and containing the most nerve fiber pathways. Essentially, the main function of the CC is to connect regions of the cerebral cortex to achieve interhemispheric integration. It also acts as a conduit to transmit

sensory information (McLeod *et al*. 1987; Byrd *et al*. 1990). It is known that structural changes in the CC are associated with neuropsychiatric symptoms such as epilepsy, Asperger's syndrome, learning disabilities, behavioral problems, depression, adjustment disorder, schizophrenia, alexithymia, delusions, hallucinations and conversion disorder (Bhatia *et al*. 2016; Randall 1983).

In the last two decades, statistical shape analysis (SSA) has been widely used in medicine to examine various structures of interest to determine morphometric features of abnormalities of an organ associated with a particular condition or disease. Offering many different methods for measuring anatomical brain structures, SSA has become a growing interest, particularly in neuroimaging. These studies often rely on measurements of volume and area, which are quantitative features that can predict the progression of disease-induced atrophy or dilation. However, structural changes occurring in certain locations may not be adequately reflected in these volume and area measurements, because it is possible for two different individuals to have the same organs in the same volume and area dimensions, but with differences in shape. Today, with technical developments, imaging views and shapes of organs or tissue structures are widely used as photographic input data. With these data, geometric shape changes in any organ or textural structure can be statistically analyzed using certain signs. SSA is a modern geometric-morphometric analysis method that can be used to evaluate the effects of demographic factors, environmental influences or diseases on growth and allometry and compares body shapes with specific anatomical features using static landmarks. This method is a form of analysis that gives more objective results with multivariate and integrated data on morphological shapes compared to analyses using classical linear measurements. SSA is increasingly used in medicine to examine various structures to identify morphometric abnormalities associated with a particular condition or disease that can aid diagnosis and treatment (Kaya *et al*. 2019; Styner *et al*. 2004; Ozdemir *et al*. 2007; He *et al*. 2010; Casanova *et al*. 2011; Joshi *et al*. 2013; Jiang *et al*. 2018; Sigirli *et al*. 2020; Huang and Tang 2021).

Studies in the literature have shown that abnormalities in the CC are associated with FND symptoms (David *et al*. 1993; Baykara *et al*. 2021). Based on this information, the aim of this study is to evaluate the CC with SSA using T1-weighted sagittal MR images of patients with FND and compare them with healthy controls.

Material and methods

Local Ethics Committee approval was obtained (date: 03/28/2013, session: 05, decision: 02) and all participants signed an informed consent form.

Study population

Twenty female patients who were diagnosed with FND according to the Diagnostic and Statistical Manual of Mental Disorders-5 (American Psychiatric Association and American Psychiatric Association DSM-5 Task Force, 2013) criteria in the psychiatry outpatient clinic and whose first symptom was psychogenic non-epileptic seizures were evaluated. The diagnosis of the patients was confirmed as a result of a psychiatric evaluation by a psychiatrist with 15 years of experience. Patients had been using selective serotonin reuptake inhibitors or tricyclic antidepressants for at least the past four months, and their doses were stabilized two months before the study. Inclusion criteria were 18-65 years of age, no other psychiatric diagnosis, no mental retardation, no neurological or physiological disease, no history of alcohol or substance use in the last 6 months, and no contraindications for magnetic resonance imaging (MRI) examination. These criteria were applied using the hospital information system and information obtained from patient statements. As the control group, 20 age and gender equivalent healthy individuals who met the study criteria and did not have a psychiatric diagnosis were selected.

Imaging process

A 1.5T General Electric Signa Excite scanner (GE, Milwaukee, Wisconsin, USA) with an 8-channel HR brain coil was used for MRI. High resolution structural T1-weighted sagittal 3D fast spin echo MRI images were obtained (TR = 2000 ms, TE = 15.6 ms, TI = 700 ms, FOV = 240 mm, echo spacing = 15.6 ms, 8 echoes, resolution = 0.9375 × 0.9375 × 1.328 mm, 128 contiguous slices). The anteroposterior commissure line and interhemispheric fissure were used to align the brains of all individuals in a standard position in MRI examinations (Fig. 1).

Analysis of images

Obtaining two-dimensional landmarks

Mid-sagittal T1-weighted two-dimensional digital MRI images of each individual, most

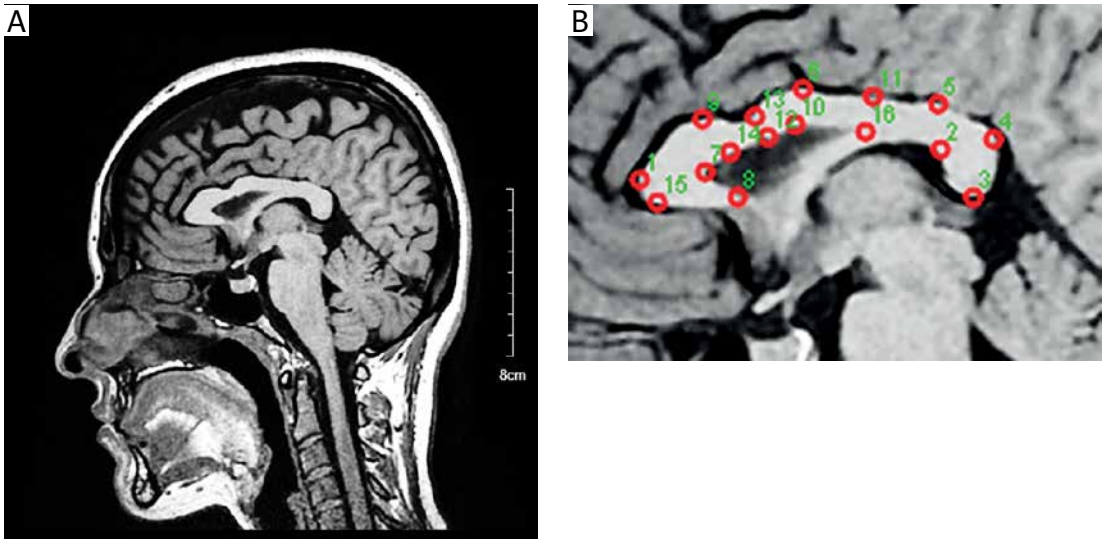

Fig. 1. A) A cross-sectional image selected from the MRI examination and B) in this image, the CC is marked with standard anatomical landmarks

clearly showing the cerebral aqueduct, CC, and superior colliculus, were selected. The corpus callosum was marked (Fig. 1) with TpsDig2 version 2.32 software on each selected image using standardized anatomical landmarks (Bookstein *et al*. 2001; Ozdemir *et al*. 2007; Sigirli *et al*. 2012) and data were collected (Rohlf 2015).

Statistical deformation analysis

The mean of 'Procrustes' landmark points was calculated and shape deformations were evaluated using thin plate spline (TPS) analysis with Past version 4.07b (Hammer *et al*. 2001). Areas that show the greatest expansion or contraction as a result of this analysis are marked using different colors to indicate deformations. The homogeneity of the variance-covariance matrices was examined using the Box-M test (Hammer *et al*. 2001; Dryden and Mardia 2016). Because of the non-homogeneous matrices, the James F_J test based on a resampling procedure was used to compare the shapes of the CC between the control and FND groups (Dryden and Mardia 2016; R Core Team 2021). In addition, the root mean square of Kendall's Riemann distance rho was compared with the mean shape to obtain overall shape variability measures for the controls and FND groups. Allometric evaluation was performed using multivariate regression analysis of centroid sizes (CS, the square root of the sum of the square of the Euclidean distances from each sign to the center) and tangent coordinates. Model significance was assessed using the Wilks' lambda test. Assessment of model fit was performed based on the mean square error (MSE) and the coefficient of determination (R^2) (He *et al*. 2010; Kaya *et al*. 2019; Sigirli *et al*. 2020).

Landmark reliability

In this study, a single rater manually defined all landmarks. Intra-rater reliability was not calculated, as the high rater reliability of landmark selection was demonstrated by previous studies (Kaya *et al*. 2019; Sigirli *et al*. 2020).

Statistical analysis

Shapes version 1.2.6 package with the R version 4.1.1 and PAST version 4.07b were used for the statistical shape analysis (Hammer *et al*. 2001; Dryden and Mardia 2016). Data were expressed as mean ± standard deviation. According to normal distribution analysis (one sample Kolmogorov-Smirnov test) of variables, Student's *t* test was used to compare the groups for other data. All statistical analyses were made with IBM SPSS Statistics (SPSS for Windows version 25, IBM Corporation, Armonk, New York, USA). A p value of < 0.05 was considered statistically significant.

Results

All patients and control subjects were female. The mean age was 32.50 ±10.47 years in the patient group and 38.45 ±10.65 years in the control group, and there was no significant difference between the groups according to age ($p = 0.083$). There was no significant difference between the CC area in the mid-sagittal images of the patients diagnosed with FND and controls

(6.01 ±0.84 cm², 5.64 ±0.69 cm² respectively; $p = 0.133$).

As the Box-M test identifies inhomogeneous matrices ($F = -0.70919$, $p < 0.001$), the James F_J test was applied and CC shapes of FND patients were found to be significantly different from controls ($T^2 = 182.1054$, $p < 0.001$) (Fig. 2). The root mean square of Kendall's Riemann distance (rho) to main shape was 0.08552594 for controls, 0.08202397 for FNDs, and 0.05922028 for all (Fig. 3).

The effect of size-dependent shape changes and deformations in the mean shape on graphs (shrinkage) was demonstrated and compared between controls and FND patients using TPS (Fig. 4). Maximum deformation was observed at marked points (landmarks) in the posterior region of the CC (especially landmarks 5, 4, 15 and 3, 8, 6, 11, 10, 1, 9, 2, 12, 13, 16, 14, and 7 in descending order) (Table 1).

The cubic growth model was chosen as the optimal model for CC and it was observed that CS for CCs decreased with increasing disease duration (Fig. 5).

The multivariate regression test was used for the relationship between size and shape in the evaluation of allometry and a statistically significant model ($p = 6.41E\text{-}40$, $R^2 = 0.08868$, MSE = 0.0002344 and Wilks' $\lambda = 3.69E\text{-}09$) was obtained for the CC.

Discussion

Until recently, for nearly two centuries, the diagnosis of functional neurological disorder was based on the inconsistency of its sensory, motor, neurovegetative symptoms with any known neurological disease. While it is thought that no anatomical or functional pathology was detected in the brains of these patients with neuroimaging, the latest study findings point to structural and functional changes in the regions of the brain associated with symptoms (Reynolds 2012; Baykara *et al*. 2021; Baykara and Baykara 2021; Byrd *et al*. 1990; Vuilleumier *et al*. 2001; Atmaca *et al*. 2006; Voon *et al*. 2011; Baumann and Mattingley 2012; Giedd *et al*. 2012; Aybek *et al*. 2014; Aybek *et al*. 2015; Atmaca *et al*. 2016; Hassa *et al*. 2017).

The CC provides integration between the hemispheres by connecting the relevant cerebral cortex regions in the brain (McLeod *et al*. 1987; Byrd *et al*. 1990). Disruption of this connection causes decreased transfer of information from one hemisphere to the other, impaired harmony between right and left visual fields, alexithymia, which is common in FND patients, delusions and hallucinations. In addition, the presence of schizophrenia, Asperger's syndrome, personality disorder, depressive symptoms and conversion symptoms in CC agenesis that is different from the others has also been reported (David *et al*. 1993; Demartini *et al*. 2014). Furthermore, the association of white matter, including CC, with psychogenic conditions has been investigated in many studies, and empirical evidence from neuroimaging studies suggests that the CC plays an important role in mood states (Wu *et al*. 1993; Huber *et al*. 2002; Lyoo *et al*. 2002; Thomas *et al*. 2002; Nery-Fernandes *et al*. 2012; Lent and Schmidt 1993; Schutter and Harmon-Jones 2013), but structural neuroimaging fails to extract information about its functionality.

Statistical shape analysis has received more attention recently for its potential to demonstrate morphological changes, but relatively few medical studies have analyzed the shape of the CC to investigate the etiology of psychiatric disorders (Kaya *et al*. 2019; Sigirli *et al*. 2020; Huang and Tang 2021).

In the present study, when examined with SSA, the CC shape of the patients was different from that of healthy controls; however, no significant difference was found between FND patients and controls in terms of CC areas in cross-sectional images.

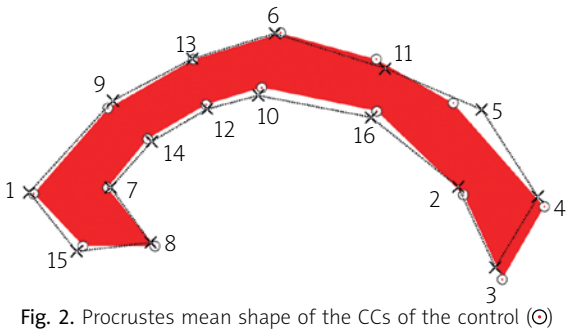

Fig. 2. Procrustes mean shape of the CCs of the control (⊙) and FND groups (×) with their landmark numbers

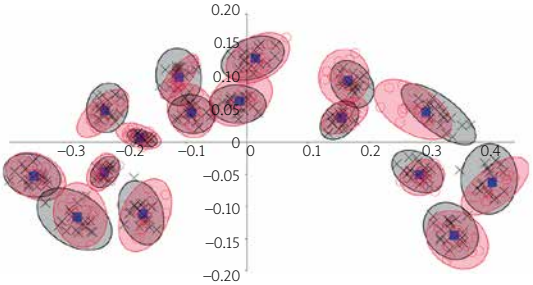

Fig. 3. Elliptical landmark scatter plots with 95% data (overall mean (■), controls (○) and FNDs (×))

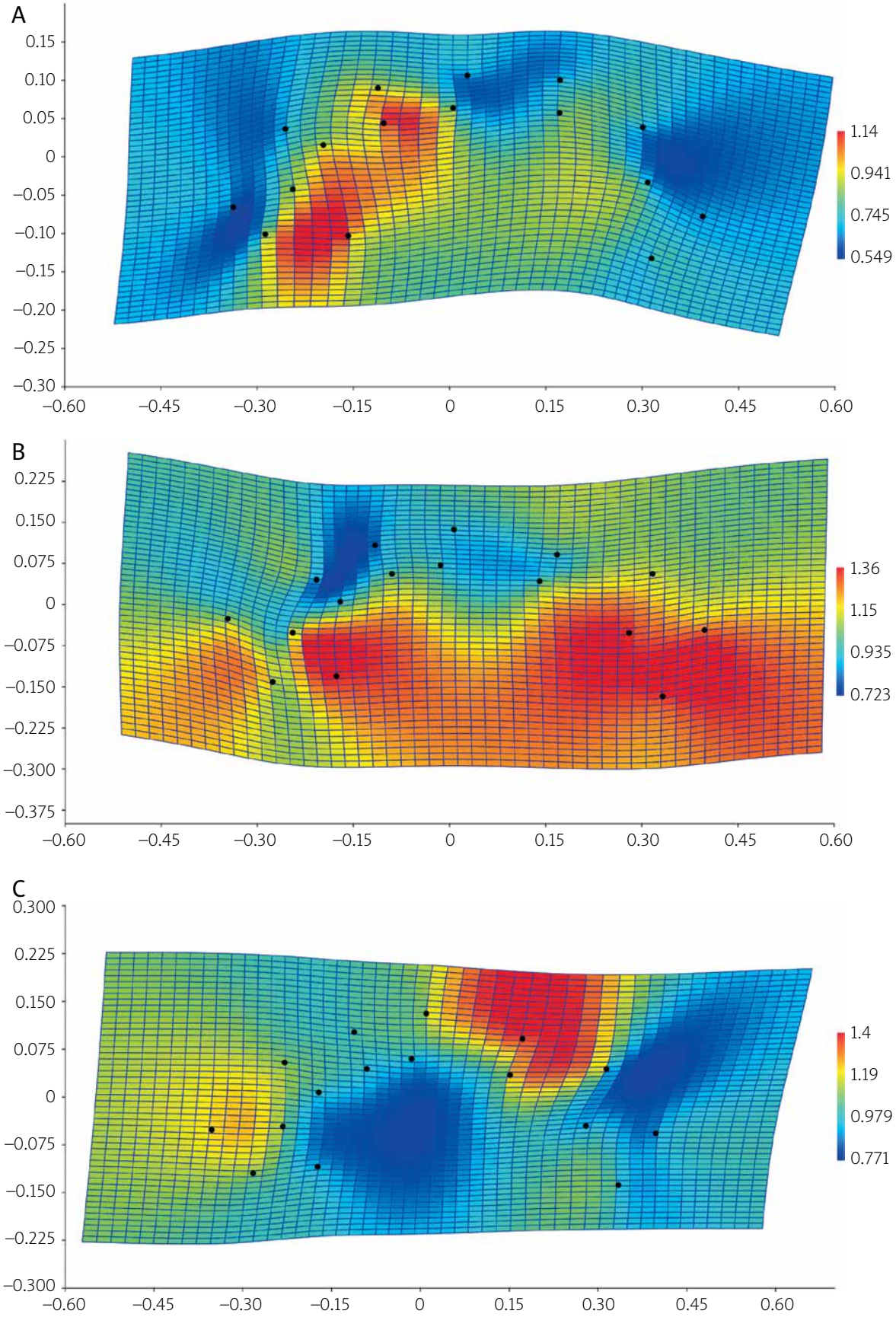

Fig. 4. Thin-plate spline transformation grid with expansion factors of the transformation from the overall mean to the control group (**A**), from the overall mean to the FND group (**B**) and from the FND group to the control group (**C**). Distortion color coding for all grid elements: color scale changing from blue for expansion to red for contraction

Table 1. Average dissimilarity values and contribution to group difference percentages of landmarks

Landmark	Dissimilarity (m)	Contribution (%)	*p*
1	0.0009405	5.38	0.0003
2	0.0007742	4.43	
3	0.0013859	7.93	
4	0.0015013	8.59	
5	0.0033256	19.03	
6	0.0010938	6.26	
7	0.0003541	2.03	
8	0.0011941	6.83	
9	0.0008555	4.90	
10	0.0010593	6.06	
11	0.0010668	6.10	
12	0.0007366	4.22	
13	0.0007077	4.05	
14	0.0003667	2.10	
15	0.0014679	8.40	
16	0.0006475	3.71	

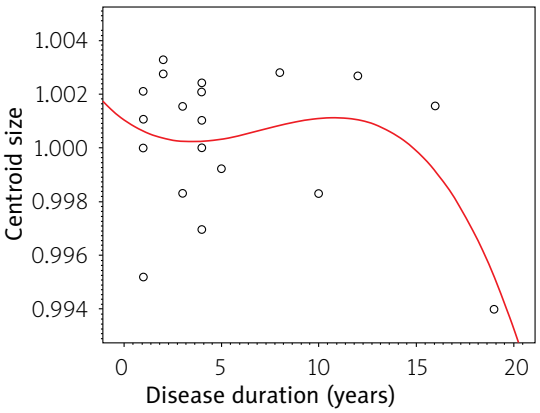

Fig. 5. Growth curve between the size of the CC's centroid and disease duration

As the assessment of general form differentiation using neuroanatomical landmarks was considered most appropriate, analyses were performed using the traditional landmark-based TPS method to examine the shape abnormalities of CC in FND in this study. To our knowledge, this study was the first to use landmark-based SSA methods to analyze CC abnormalities in FND, and local shape comparison had not been performed before.

Some studies using shape analysis have reported significant findings about various CC subdivisions, such as in Alzheimer's disease, where the CC is globally atrophic and this is more prominent in the posterior segment, and the lower border is longer than the upper margin; in autism, there are differences in the body segment of CC; and in multiple sclerosis, there are differences in body and anterior segments of CC. Regional distribution differences of CC injury should result from variable regional fiber amounts associated with different neuroanatomical regions (He *et al*. 2010; Sigirli *et al*. 2012; Sigirli *et al*. 2020; Jiang *et al*. 2018; Walterfang *et al*. 2014).

In this study, it was determined that the maximum deformation was located in the posterior region (isthmus and splenium), inferior edge of the body and anterior region (genu) of the CC. The first two CC regions connect temporal (especially superior), occipital, parietal and motor activation cortical areas (landmarks = 11, 5, 4, 3, 2, 16 and 10). They are also predominantly areas of tactile, auditory, and peripheral and central visual stimulation. The genu connects prefrontal and cingulate areas, which are associated with cognitive information (landmarks 15 and 1) (Friedrich *et al*. 2020; Fabri and Polonara 2013; Chao *et al*. 2009; Hofer and Frahm 2006).

Limitations

The present study had certain limitations. Since there were no previous studies that analyzed CC with SSA in patients with FND, we were not able to compare the study findings. The fact that all our patients were female prevented the generalization of the study findings to both sexes. The small sample size of patients and controls was another limitation of the study. Although morphological evaluation with 3D data may seem difficult now, it is certain that it will give results that are more accurate in the morphological analysis of organs in spatial dimensions. In addition, study participants had been taking antidepressant medications, specifically selective serotonin reuptake inhibitors, for the past few months. Although it has been shown in animal models that the physiology of serotonin in CC is impaired by antidepressant drugs (Reyes-Haro *et al*. 2003), the effects of antidepressants on CC have not been well studied and further studies are needed in this regard.

Conclusions

In this study, SSA and CC analysis using MRI images revealed significant differences between patients with FND and healthy controls. The study findings highlighted the abnormal distribution of white matter in the CC and the variable subregional nature of the CC in FND

patients. Future studies with larger samples may contribute to further elucidation of these findings. This study may help future studies in terms of FND etiology, diagnosis and treatment options.

Disclosure

The authors declare no conflict of interest.

References

1. American Psychiatric Association DSM-5 Task Force. Diagnostic and statistical manual of mental disorders: DSM-5. American Psychiatric Association, Washington, D.C. 2013.
2. American Psychiatric Association. Diagnostic and statistical manual of mental disorders (DSM-5®). American Psychiatric Pub. 2013.
3. Atmaca M, Aydin A, Tezcan E, et al. Volumetric investigation of brain regions in patients with conversion disorder. Prog Neuropsychopharmacol Biol Psychiatry 2006; 30: 708-713.
4. Atmaca M, Baykara S, Mermi O, et al. Pituitary volumes are changed in patients with conversion disorder. Brain Imaging Behav 2016; 10: 92-95.
5. Aybek S, Nicholson TR, Draganski B, et al. Grey matter changes in motor conversion disorder. J Neurol Neurosurg Psychiatry 2014; 85: 236-238.
6. Aybek S, Nicholson TR, O'Daly O, et al. Emotion-motion interactions in conversion disorder: an FMRI study. PLoS One 2015; 10: e0123273.
7. Baumann O, Mattingley JB. Functional topography of primary emotion processing in the human cerebellum. Neuroimage 2012; 61: 805-811.
8. Baykara M, Baykara S. Texture analysis of dorsal striatum in functional neurological (conversion) disorder. Brain Imaging Behav 2022; 16: 596-607.
9. Baykara S, Baykara M, Mermi O, et al. Magnetic resonance imaging histogram analysis of corpus callosum in a functional neurological disorder. Turk J Med Sci 2021; 51: 140-147.
10. Bhatia MS, Saha R, Doval N. Delusional disorder in a patient with corpus callosum agenesis. J Clin Diagn Res 2016; 10: VD01-VD02.
11. Bookstein FL, Sampson PD, Streissguth AP, et al. Geometric morphometrics of corpus callosum and subcortical structures in the fetal-alcohol-affected brain. Teratology 2001; 64: 4-32.
12. Byrd SE, Radkowski MA, Flannery A, et al. The clinical and radiological evaluation of absence of the corpus callosum. Eur J Radiol 1990; 10: 65-73.
13. Casanova MF, El-Baz A, Elnakib A, et al. Quantitative analysis of the shape of the corpus callosum in patients with autism and comparison individuals. Autism 2011; 15: 223-238.
14. Chao YP, Cho KH, Yeh CH, et al. Probabilistic topography of human corpus callosum using cytoarchitectural parcellation and high angular resolution diffusion imaging tractography. Hum Brain Mapp 2009; 30: 3172-3187.
15. David AS, Wacharasindhu A, Lishman WA. Severe psychiatric disturbance and abnormalities of the corpus callosum: review and case series. J Neurol Neurosurg Psychiatry 1993; 56: 85-93.
16. Demartini B, Petrochilos P, Ricciardi L, et al. The role of alexithymia in the development of functional motor symptoms (conversion disorder). J Neurol Neurosurg Psychiatry 2014; 85: 1132-1137.
17. Dryden IL, Mardia KV. Statistical shape analysis with applications in R. Hoboken, NJ, Wiley, Chichester, UK 2016.
18. Fabri M, Polonara G. Functional topography of human corpus callosum: an FMRI mapping study. Neural Plast 2013; 2013: 251308.
19. Friedrich P, Forkel SJ, Thiebaut De Schotten M. Mapping the principal gradient onto the corpus callosum. Neuroimage 2020; 223: 117317.
20. Giedd JN, Raznahan A, Mills KL, et al. Review: magnetic resonance imaging of male/female differences in human adolescent brain anatomy. Biol Sex Differ 2012; 3: 19.
21. Hammer Ø, Harper DA, Ryan P. Paleontological statistics software package for education and data analysis. Paleontologia Electronica 2001; 4: 1-9.
22. Hassa T, Sebastian A, Liepert J, et al. Symptom-specific amygdala hyperactivity modulates motor control network in conversion disorder. Neuroimage Clin 2017; 15: 143-150.
23. He Q, Duan Y, Karsch K, et al. Detecting corpus callosum abnormalities in autism based on anatomical landmarks. Psychiatry Res 2010; 183: 126-132.
24. Hofer S, Frahm J. Topography of the human corpus callosum revisited – comprehensive fiber tractography using diffusion tensor magnetic resonance imaging. Neuroimage 2006; 32: 989-994.
25. Huang W, Tang X. Down-sampling template curve to accelerate LDDMM-curve with application to shape analysis of the corpus callosum. Healthc Technol Lett 2021; 8: 78-83.
26. Huber M, Herholz K, Habedank B, et al. Different patterns of regional brain activation during emotional stimulation in alexithymics in comparison with normal controls. Psychother Psychosom Med Psychol 2002; 52: 469-478.
27. Jiang Z, Yang H, Tang X. Deformation-based statistical shape analysis of the corpus callosum in mild cognitive impairment and Alzheimer's disease. Curr Alzheimer Res 2018; 15: 1151-1160.
28. Joshi SH, Narr KL, Philips OR, et al. Statistical shape analysis of the corpus callosum in schizophrenia. Neuroimage 2013; 64: 547-559.
29. Kaya MO, Ozturk S, Ercan I, et al. Statistical shape analysis of subthalamic nucleus in patients with Parkinson disease. World Neurosurg 2019; 126: e835-e841.
30. Lent R, Schmidt SL. The ontogenesis of the forebrain commissures and the determination of brain asymmetries. Prog Neurobiol 1993; 40: 249-276.
31. Lyoo IK, Kwon JS, Lee SJ, et al. Decrease in genu of the corpus callosum in medication-naive, early-onset dysthymia and depressive personality disorder. Biol Psychiatry 2002; 52: 1134-1143.
32. Mcleod NA, Williams JP, Machen B, et al. Normal and abnormal morphology of the corpus callosum. Neurology 1987; 37: 1240-1242.
33. Nery-Fernandes F, Rocha MV, Jackowski A, et al. Reduced posterior corpus callosum area in suicidal and non-suicidal patients with bipolar disorder. J Affect Disord 2012; 142: 150-155.
34. Ozdemir ST, Ercan I, Sevinc O, et al. Statistical shape analysis of differences in the shape of the corpus callosum between genders. Anat Rec (Hoboken) 2007; 290: 825-830.
35. R Core Team. R: A language and environment for statistical computing. R Foundation for Statistical Computing, Vienna, Austria. URL http://www.R-project.org/.
36. Randall PL. Schizophrenia, abnormal connection, and brain evolution. Med Hypotheses 1983; 10: 247-280.

37. Reyes-Haro D, Garcia-Alcocer G, Miledi R, et al. Uptake of serotonin by adult rat corpus callosum is partially reduced by common antidepressants. J Neurosci Res 2003; 74: 97-102.
38. Reynolds EH. Hysteria, conversion and functional disorders: a neurological contribution to classification issues. Br J Psychiatry 2012; 201: 253-254.
39. Rohlf FJ. The tps series of software. Hystrix. Italian J Mammalogy 2015; 26: 9-12.
40. Schutter DJ, Harmon-Jones E. The corpus callosum: a commissural road to anger and aggression. Neurosci Biobehav Rev 2013; 37: 2481-2488.
41. Sigirli D, Ercan I, Ozdemir ST, et al. Shape analysis of the corpus callosum and cerebellum in female MS patients with different clinical phenotypes. Anat Rec (Hoboken) 2012; 295: 1202-1211.
42. Sigirli D, Gunes A, Turan Ozdemir S, et al. Statistical shape analysis of corpus callosum in restless leg syndrome. Neurol Res 2020; 42: 760-766.
43. Styner M, Lieberman JA, Pantazis D, et al. Boundary and medial shape analysis of the hippocampus in schizophrenia. Med Image Anal 2004; 8: 197-203.
44. Thomas AJ, Perry R, Barber R, et al. Pathologies and pathological mechanisms for white matter hyperintensities in depression. Ann N Y Acad Sci 2002; 977: 333-339.
45. Voon V, Brezing C, Gallea C, et al. Aberrant supplementary motor complex and limbic activity during motor preparation in motor conversion disorder. Mov Disord 2011; 26: 2396-2403.
46. Vuilleumier P, Chicherio C, Assal F, et al. Functional neuroanatomical correlates of hysterical sensorimotor loss. Brain 2001; 124: 1077-1090.
47. Walterfang M, Luders E, Looi JC, et al. Shape analysis of the corpus callosum in Alzheimer's disease and frontotemporal lobar degeneration subtypes. J Alzheimers Dis 2014; 40: 897-906.
48. Wu JC, Buchsbaum MS, Johnson JC, et al. Magnetic resonance and positron emission tomography imaging of the corpus callosum: size, shape and metabolic rate in unipolar depression. J Affect Disord 1993; 28: 15-25.